Biosynthesized silver nanoparticles (using Cinnamomum zeylanicum bark extract) improve the fertility status of rats with polycystic ovarian syndrome

Article *in* Biocatalysis and Agricultural Biotechnology · November 2021

DOI: 10.1016/j.bcab.2021.102217

CITATIONS
13

READS
419

2 authors:

Muna Hameed AL-Saeed
University of Basrah, College of Veterinary Medicine
106 PUBLICATIONS **132** CITATIONS
SEE PROFILE

Shukrya H. Alwan
Al-Furat Al-Awsat Technical University
8 PUBLICATIONS **60** CITATIONS
SEE PROFILE

Biocatalysis and Agricultural Biotechnology xxx (xxxx) 102217

Contents lists available at ScienceDirect

Biocatalysis and Agricultural Biotechnology

journal homepage: www.elsevier.com/locate/bab

Biosynthesized silver nanoparticles (using *Cinnamomum zeylanicum* bark extract) improve the fertility status of rats with polycystic ovarian syndrome

Shukrya H. Alwan [a, b, *], Muna H. Al-Saeed [a]

[a] Department of Physiology, Pharmacology and Biochemistry, College of Veterinary Medicine, University of Basrah, Basrah, Iraq
[b] Department of Community Health, Technical Institute of Karbala, Al-Furat Al-Awsat Technical University, Karbala, Iraq

ARTICLE INFO

Keywords:
Cinnamon
Estradiol valerate
Fertility
Hormones
Polycystic ovarian syndrome
Silver nanoparticles

ABSTRACT

This study is aimed to investigate the effectiveness of biosynthesized silver nanoparticles (AgNPs) on the fertility status of female rats with estradiol valerate (EV)-induced polycystic ovarian syndrome (PCOS). AgNPs were synthesized using *C. zeylanicum* extract and characterized by SEM, AFM, FTIR, XRD, zeta potential and UV–Vis spectroscopy. Fifty female rats were divided into five groups (n = 10). The control groups were vehicle control (GI, received corn oil of 0.2 ml only) and PCOS control (GII, received EV only). While, the treatment groups were GIII (treated with *C. zeylanicum* methanolic extract 200 mg/kg body weight), GIV (treated with metformin 50 mg/kg body weight) and GV (treated with 3.53 mg/kg body weight biosynthesized AgNPs). The treatment duration was 30 days. The protective effects of these treatments against PCOS were assessed by routine vaginal smear examination, sex hormones levels (LH, FSH, E2, progesterone and testosterone), histopathologic features and the fertility rate. When compared with PCOS rats, AgNPs treatment increased serum FSH and progesterone levels and decreased E2 and testosterone significantly. Histopathologic examination showed that the EV-induced PCOS group developed polycysts in their ovaries and those changes reduced or disappeared in the treated groups. Moreover, the treatment with *C. zeylanicum* extract and AgNPs have effectively improved the estrus cycle as well as the fertility rate in treated groups compared with PCOS group. Our findings suggest that biosynthesized AgNPs can improve the fertility rate and estrous cycle by regulating sex hormones involved in the pathogenesis of PCOS.

1. Introduction

Polycystic ovarian syndrome (PCOS) is one of the most prevalent hormonal imbalance diseases affecting 5–20% of women at reproductive age in the world. It is characterized by polycystic ovarian morphology, hyperandrogenism, hirsutism, menstrual irregularity, ovarian dysfunction and infertility (Azziz et al., 2016; Duleba, 2012; Rostamtabar et al., 2021). About 50%–70% of anovulatory infertility cases were reported to be linked to PCOS (Teede et al., 2008), especially those accompanied by a low ovulation induction rate, low pregnancy rate, and high abortion rate. One of the main causes of anovulatory infertility, in reproductive-aged women, is hyperandrogenism (especially hypertestosteronaemia) which results in a lack of ovulation and irregular sex hormone synthesis (Abasian et al., 2018). Increased luteinizing hormone (LH) and comparatively lower follicle-stimulating hormone (FSH), as well as overproduction of ovarian androgens, result in an abnormal ovarian cycle (Azarnia et al., 2015). PCOS is associated with several

* Corresponding author. Department of Physiology, Pharmacology and Biochemistry, College of Veterinary Medicine, University of Basrah, Basrah, Iraq.
E-mail address: shuk_hat11290@yahoo.com (S.H. Alwan).

https://doi.org/10.1016/j.bcab.2021.102217
Received 9 May 2021; Received in revised form 30 August 2021; Accepted 9 November 2021
1878-8181/

other metabolic disorders, including insulin resistance (IR), diabetes, cardiovascular disease, and obesity. Although previous evidence suggest that the lifestyle, neuroendocrine, genetic factors, immune and metabolic dysfunction may be involved in the pathogenesis of PCOS (Nasser et al., 2019; Rosenfield and Ehrmann, 2016), the exact etiology is still unclear.

In recent years, nanotechnology has extremely been used in almost all fields of science and technology. In biomedicine, many applications of nanomaterials in the diagnosis and treatment have been reported (Jasim et al., 2020). Silver nanomaterials have gained great attention in past two decades, because the silver nanoparticles (AgNPs) were reported to have antioxidant, antimicrobial, and anti-inflammatory effects (Burduşel et al., 2018; Keshari et al., 2020; Sriramulu and Sumathi, 2017). In 2018, Salami et al. found that AgNPs can assist in the treatment of PCOS through the protection of hypothalamus.

Several methods are there to prepare nano materials (Burduşel et al., 2018). Apart from chemical and physical methods who seem hazardous and very expensive, green synthesis method of nanomaterials can result in high-yield, high-stability and solubility nanoparticles (Gurunathan et al., 2015). In green synthesis (or biosynthesis) of nanoparticles, plant extracts are used because their contents of phytochemicals (secondary metabolites) are directly involved in the reduction of metal ions and the formation of nanoparticles (Abbasi et al., 2016; Ingale and Chaudhari, 2013). On the other hand, some plants are well known and described for centuries as "medicinal plants" because they have distinct remedy effectiveness (Yaseen et al., 2020). In this respect, *Cinnamomum zeylanicum* (cinnamon, abbreviated as CZ) is a medicinal plant with various therapeutic effects since it was described for respiratory, gynecological, and digestive ailments since ancient (Ranasinghe et al., 2013). Current hypotheses for interpreting the medicinal activities of CZ suggest that such activities can be ascribed to its content of bioactive constituents such as polyphenolic compounds. The major active compound of CZ is cinnamaldehyde, which has many health benefits such as antioxidant, anti-diabetic, antimicrobial, anti-inflammatory and anti-gastric ulcer effects (Dorri et al., 2018). Thus, it can be hypothesized that the use of medicinal plants in the biosynthesis of nanoparticles can strengthen its therapeutic efficiency.

Estradiol valerate (EV)-induced PCOS experimental models show similar characteristics to those seen in human patients such as irregularities in the estrus cycle (EC), hormone abnormalities, abnormal maturation of ovarian follicles, development of ovarian cyst, and anovulation (Azarnia et al., 2015). Therefore, testing the new therapeutic agents on rat model with EV-induced PCOS can offer acceptable outcomes to draw valid conclusions.

Abdalla et al. (2015) showed that the green synthesis of AgNPs (using the CZ) is quick and result in safe and stable nanomaterials can be used in various biomedical applications. Up to date, no study about the effectiveness of biosynthesized AgNPs on the PCOS was published. Accordingly, we hypothesized that the green synthesis of AgNPs can improve the fertility status in EV-induced PCOS rats. Thus, the current study is sought to investigate the influence of biosynthesized AgNPs (using CZ bark extract) on sex hormones, EC, histopathologic features, and the fertility rate of EV-induced PCOS rats.

2. Materials and methods

2.1. Biosynthesis and characterization of AgNPs

2.1.1. Preparation of CZ bark extract

The extract was prepared by adding approximately 20g of fine powder of CZ barks in the Soxhlet's apparatus (Thumble) with 100 ml of 80% hydro-methanol (water:methanol, 20:80 v/v). The extraction was performed at 80°C for 8–10 h. The extract was then filtered and concentrated on a rotary evaporator until it became completely dry (Mariappan et al., 2013).

2.1.2. Fabrication of AgNPs

Silver nanoparticles (AgNPs) were prepared using the green method described by Gauthami et al. (2015) with slight modifications. Five milliliters of the extract, of CZ bark, were added gradually drop-by-drop to 200 ml of 1 mM silver nitrate ($AgNO_3$) under ultrasound conditions for 30min. After that, the mixture was shaken for 20min with a magnetic stirrer, then stored for 72h in dark conditions. The color change from reddish-brown to dark brown during 72h indicated the formation of AgNPs. Finally, at 10,000 rpm (for 10min at 4°C), the sample was centrifuged and the suspension was washed 5 times repeatedly (Gauthami et al., 2015) to eliminate non-nano materials. All chemicals were purchased from Sigma-Aldrich, Germany.

2.1.3. Characterization of AgNPs

The biosynthesis of AgNPs was monitored periodically in a UV–visible spectrophotometer (Biotech-LTD, UK), in the scan range wavelength of 200–800 nm. Scanning electron microscopy (SEM, VEGAIII, Czech Republic) was used to observe the morphology of AgNPs. In addition, atomic force microscopy (AFM, Negara, Russian Federation) was used to determine the nano-sizes of Ag particles as well as many other physical properties. Fourier transforms infrared spectroscopy analysis (FTIR, Shemadzu8400s, Japan) was used for detecting the active compounds present in the CZ extract that are involved in the reduction of Ag^+ ions. The FTIR analysis was carried out with a resolution of 4 cm^{-1} in 400–4000 cm^{-1}. Nanoparticles' stability and their surface charge were studied by zeta potential analysis (Brookhaven, USA). Its measurement was performed at a field strength of 20 V/cm and at a temperature of 25°C. The zeta potential analysis allows flowing from −160 mV to +160 mV and plots the data with a graph. The X-ray diffraction (XDR) technique was applied to probe the structure of AgNPs and crystalline nature at 2θ angle by Cu-Kα radiation operated at 10 kV and 30 mA. The JCPDS card reference was used for the interpretation of XRD (Wong-Ng et al., 2001). The crystallite size of AgNPs was calculated by using the Debye Scherrer equation (Sankar et al., 2013).

$$D = \frac{K\lambda}{\beta \cos\theta} \quad (1)$$

whereas, D = diameter of NPs dimension, K = a constant value (0.94 is used along with cubic symmetry to harmonize spherical crystallites), λ is the X-ray wavelength, β = Full Width at Half Maximum (FWHM) and θ (Bragg angle) = angle of diffraction.

2.2. Experimental animals

A total of 50 adult female *Rattus norvegicus* rats (12–14 weeks old, weighing 175–200g) and ten adult male rats were selected for the current study and maintained in the animal house of the College of Veterinary Medicine. The rats were housed in polypropylene cages lined with husk in standard environmental conditions (temperature 25 ± 2°C, relative humidity 55 ± 10%) and constant light/dark cycle. The rats were fed on a standard pellet diet (Amrut rat and mice feed, Syria) and water *ad libitum*. This study and its protocols are approved by the College of Veterinary Medicine (No: 3/18-01/07/2019).

2.3. Induction of PCOS

Before the beginning of the current study, daily vaginal smear tests were performed for all the 50 female rats and showed regular EC. The PCOS was induced in 40 female rats using a single intramuscular injection of EV (Sigma-Aldrich, Germany) with a dose of 4 mg/kg body weight dissolved in 0.2 ml corn oil (Sigma-Aldrich, Germany). All the Forty rats were left for 8 weeks after the day of EV injection (Jelodar et al., 2018). As a vehicle control group, ten female rats were given 0.2 ml of corn oil.

2.4. Determination of estrus cycle (EC)

For the determination of EC phases and to assess the EC regularity, the daily vaginal smear examination was conducted for each rat (Matsuzaki et al., 2017). Briefly, vaginal secretions were collected using a cotton-tipped swab with a drop of normal saline. The vaginal smears were prepared immediately, a cotton-tipped swab was rolled on the length of a clean glass slide as soon as the smears were prepared and allowed to dry. To fix the cells, few drops of methanol were added to the smear. The smears were then stained by Giemsa stain (JOURILABS, Ethiopia) by flooding them with the stain solution for 10–15min, and then; they were washed, air-dried and examined under the light microscope 40X objectives (Reddy et al., 2016). The smear was microscopically assessed for predominant nucleated epithelial cells and some cornified epithelial cells indicated the proestrus stage; predominant cornified squamous epithelial cells indicated the estrus stage; both cornified squamous epithelial cells and leukocytes indicated the metaestrus stage, and predominant leukocytes indicated the diestrus stage (Matsuzaki et al., 2017).

2.5. Experimental design

The 50 female rats were grouped into five groups (n = 10). The control groups were vehicle control (GI, received corn oil of 0.2 ml only) and PCOS control (GII, received EV only). While, the treatment groups were GIII (treated with CZ methanolic extract 200 mg/kg body weight), GIV (treated with metformin 50 mg/kg body weight) and GV (treated with 3.53 mg/kg body weight biosynthesized AgNPs). The safety of biosynthesized AgNPs used in the treatment was evidenced in our recent paper (Alwan et al., 2021). The treatment duration was 30 days. At the end of the experiment, blood and tissue samples were collected from all animals at the estrus phase, because animals in the case of EV-induced PCOS are dominant at this stage (many cornified cells) (Mohammed et al., 2021); to ensure that the biomarkers' assessment at the same phase for all animals.

2.6. Biochemical parameters (hormones)

The effects of CZ methanol bark extract, the biosynthesized AgNPs and standard drug metformin on the EV-induced PCOS were evaluated 30 days after treatment (after the animals were sacrificed, n = 6). Blood was collected from each rat by heart puncture. Serum was separated by centrifugation at 3,500 × *g* for 10min at 25°C. Serum Luteinizing Hormone (LH), Follicle Stimulating Hormone (FSH), Estradiol (E2), Progesterone (PRG) and Testosterone (TEST) levels were determined by ELISA technique using commercial test kits (Monobind Inc., USA). Testing procedures were according to the manufacturer's instructions.

2.7. Reproductive efficiency

The fertility rate was monitored and recorded in all groups. The four remaining female rats, after scarifying 6 rats, in each group were mated with male rats (2 males for each group) for the first 4 weeks after the treatment is ended (after 30 days). All pregnancies and births were then monitored and recorded in order to evaluate how the reproductive efficiency may affect by the treatment.

$$Reproductive\ rate_{(Group\ X)} = \frac{Number\ of\ pregnant\ female}{Total\ number\ of\ females} \times 100\%$$

2.8. Histopathologic features

After each rat was sacrificed, the ovaries were separated from the body to evaluate the histologic changes of ovaries for the study groups. Then, they were fixed in formalin (10%), dehydrated with alcohol, cleared with xylene, infiltrated with molten wax, blocked and finally trimmed with a microtome. The floated slices of trimmed specimens were stained with hematoxylin and eosin staining (H&E) stain. The stained slides of ovarian tissues were examined microscopically (4X).

2.9. Statistical analyses

Graph Pad Prism 8.0 (GraphPad Software, CA, USA) was used to evaluate the data, statistically. Mean ± SD were used to express the numerical data. Data was analysed using the one-way ANOVA test or Kruskal-Wallis test to assess the difference in means. A suitable post-hoc test was also used for multiple comparisons. A p-value of ≤ 0.05 was considered statistically significant.

3. Results

3.1. AgNPs synthesis and characterization

Parveen and Rao (2015) stated that the enhancement in nanoparticles' synthesis is associated with the increased color intensity of incubated nanomaterial. Thus, the biosynthesis of Ag nanomaterials in the present study was preliminarily expected by the color change after the procedure was finished. At the beginning, the $AgNO_3$ solution was colorless (Fig. 1A) and its color became yellow about 20min after the addition of CZ extract (Fig. 1B). After 1 h, the color was changed to reddish-brown (Fig. 1C) and to brown after 24h (Fig. 1D). Finally, the solution's color became dark-brown after 72h (Fig. 2) which predicts the fabrication of Ag nanomaterials. The AgNPs can be synthesized by the reduction of silver metal ions (Ag^+) into Ag^0, whereas the reducing agents are the bioactive constituents of CZ extract. Thus, a high yield of AgNPs can be gained when the duration of mixing the Ag ions and CZ is increased. Therefore, the current study demonstrated that the CZ bark extract is a good source for the synthesis of stable AgNPs in less time.

After 72h, the dark-brown color solution was centrifuged for material characterization. The optical absorbance of biosynthesized nanomaterials was measured by using UV–Vis spectroscopy (200–800 nm), at a resolution of 1 nm. Different peaks of absorbance values between (214–428 nm) were observed in the current study (Fig. 3). A distinct peak was observed at 428 nm which indicates the reduction of Ag ions.

The size and morphology of biosynthesized AgNPs were determined by SEM and AFM. The SEM image of Ag nanomaterials (Fig. 4) showed smooth, spherical particles with nano-scale sizes (different NPs' sizes appear in the SEM image, such as 45 nm, 52 nm, 60 nm, and 74 nm). A very little amount of large NPs was also seen due to aggregation. Moreover, the results of AFM analysis (Fig. 5 and Fig. 6) showed a two-dimensional view. In which, the AgNPs were spherical in shape with a singular or aggregated forms. The size of the AgNPs was ranged from 60 to 80 nm.

Next, the FT-IR analysis was carried out to identify the putative bioactive secondary metabolites present in the extract which are involved in the AgNPs synthesis and stabilization. FT-IR spectrum for AgNPs was obtained in the range of 400-4000 cm^{-1} (Fig. 7). The appearance of a broad and strong absorption band of AgNPs around (3427.51 cm^{-1}) and (3414 cm^{-1}) was assigned to the hydroxyl group (O–H) stretching vibration of phenols and alcohols. While absorption peak at(2920.23 cm^{-1}) was allocated to the carbon hydroxyl (C–H) stretching vibration of alkane. The band at (1762.94 cm^{-1}) and (1627.92 cm^{-1}) showed a nonlinear increase in the intensity which was associated with the stretching vibration of an aldehyde carbony1 C = O groups of alkenes. The peak at (1382.92 cm^{-1}) is attributed to the C–H bending in alkanes. However, the peak at (825.53 cm^{-1}) and (759.95 cm^{-1}) confirm C–X stretching in alkyl halides. Finally, the band at (667.37 cm^{-1}), (650.01 cm^{-1}) and (601.79 cm^{-1}) were due to C–N–C bending in amines. These results together confirmed the presence of functional groups in the biosynthesized AgNPs.

Fig. 8 shows AgNPs with an average zeta potential of −23.07 mV. The zeta potential is an important physical property of the particles in colloidal solution.

The green synthesis of AgNPs was further supported by X-ray diffraction (XRD) analysis. In Fig. 9, the results showed four obvious diffraction peaks at 2θ values 36.4, 43.5, 54.3, 75.1 for AgNPs which were corresponded to 111, 200, 220 and 311 planes of silver.

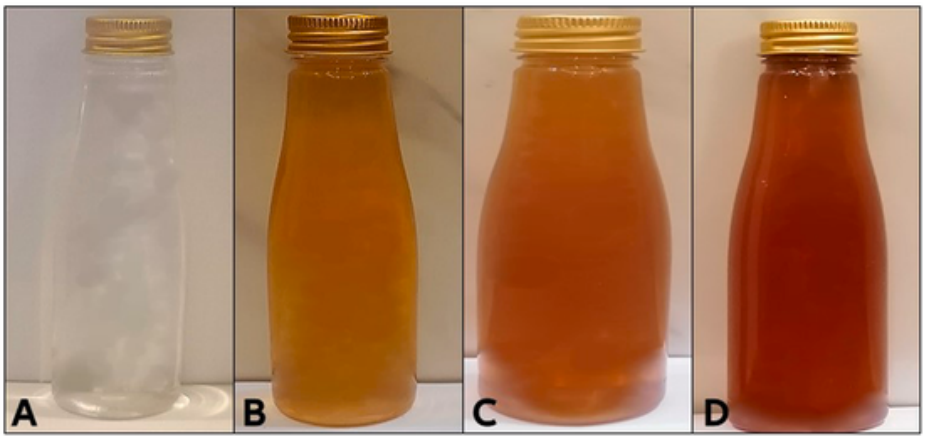

Fig. 1. Color change of $AgNO_3$ solution after adding *C. zeylanicum* (CZ) bark extract. **A)** $AgNO_3$ solution (1 mM), **B)** Yellowish color after 20 min of preparation, **C)** Reddish brown color after 1h of preparation, and **D)** Brown color after 24 h of preparation. (For interpretation of the references to color in this figure legend, the reader is referred to the Web version of this article.)

Fig. 2. Dark brown color of prepared materials after 72 h of preparation. (For interpretation of the references to color in this figure legend, the reader is referred to the Web version of this article.)

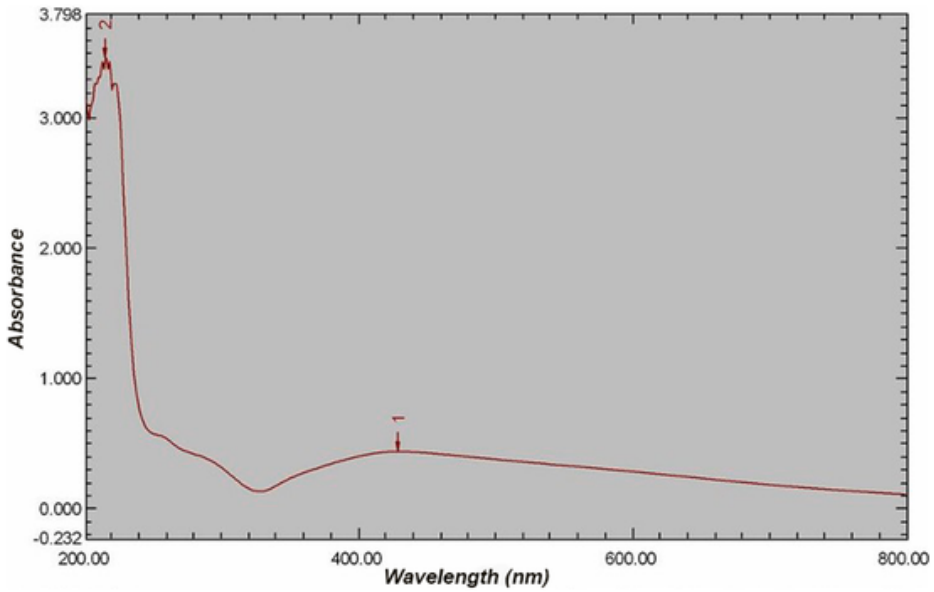

Fig. 3. UV–Vis spectrum of prepared Ag nanomaterials after 72 h of incubation.

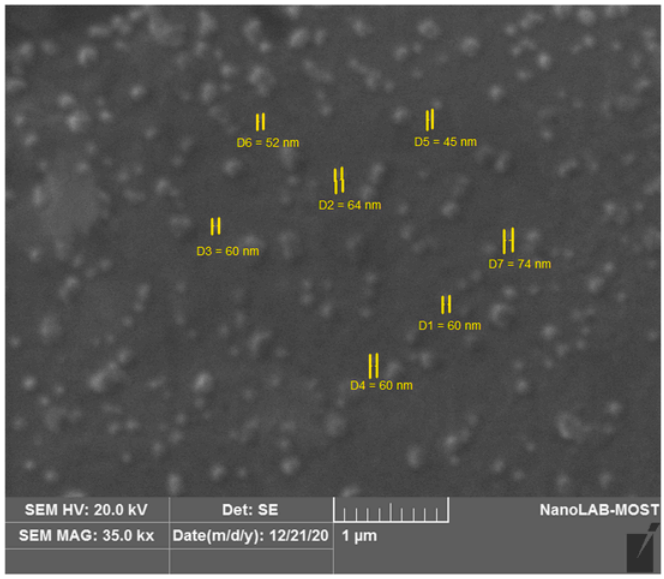

Fig. 4. Scanning electron microscopy (SEM) shows the shape and size of AgNPs.

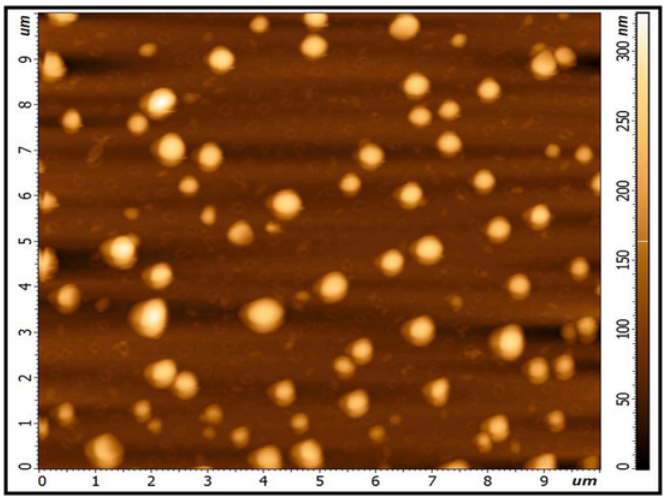

Fig. 5. AFM image showed two-dimensional view of AgNPs.

3.2. Determination of EC

The abnormal EC in the experimental groups was observed by daily vaginal smears examination as the first step in the development of PCOS. The rats in the vehicle control group are in the diestrus phase, which is characterized by prominent leukocytes with regular EC. The EC in the PCOS group was irregular and long mostly with the estrus phase showing cornified cells as compared to the vehicle control group. Regular cycles were defined as those lasting 4–5 days. However, persistent vaginal cornification (PVC) was defined as the presence of cornified cells in the smears for a minimum of 10 serial days and is an indicator of follicular cystic development. The experimental treated groups showed normal ECs. In the groups treated with CZ bark extract, the cornified and nucleated cornified squamous epithelial cells and leukocytes indicated metaestrus phase. The metformin-treated group in the present study is in the diestrus phase with the presence of leukocytes. The groups treated with AgNPs had a higher percentage of nucleated cells of the proestrus phase. Changes in the EC are represented in Fig. 10(A-D).

3.3. Biochemical parameters (hormones)

In order to evaluate the effect of biosynthesized AgNPs on EV-induced PCOS rats, the levels of FSH, LH, E2, PROG and TEST were determined in serum samples 30 days after treatment. The LH, FSH, E2, PROG, and TEST concentrations of the vehicle control group, PCOS group as well as PCOS groups who treated with various treatments are depicted in Fig. 11. The LH level was significantly increased in the PCOS group compared to the vehicle control group (0.70 ± 0.10 *vs*. 0.56 ± 0.08 mIU/ml, $p = 0.04$). In contrast, the results of the LH in the experimental groups after treatment appears to decline as compared with the positive control group (PCOS un-

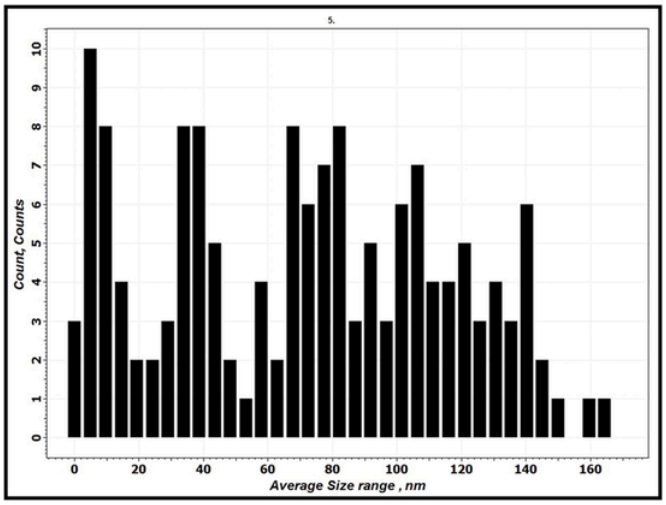

Fig. 6. AFM diagram showed the size range of AgNPs.

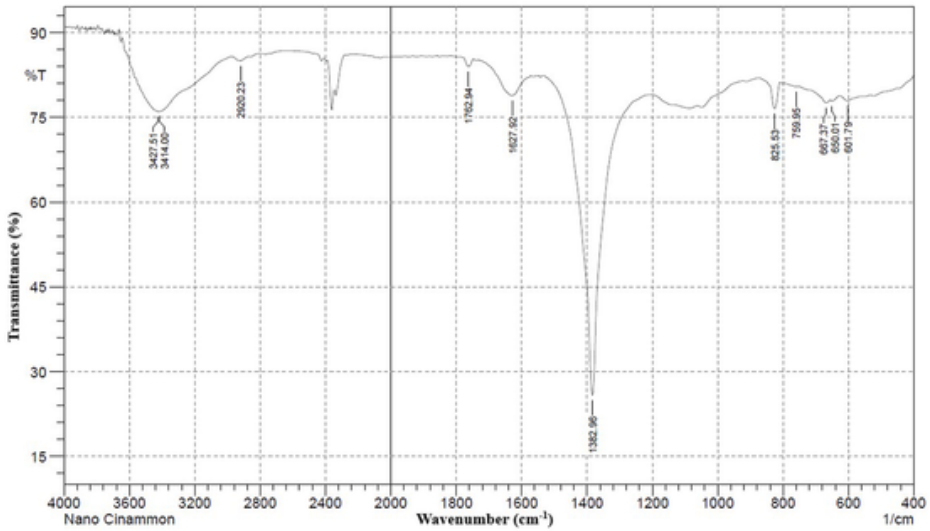

Fig. 7. FT-IR spectrum showing functional groups of biofabricated AgNPs.

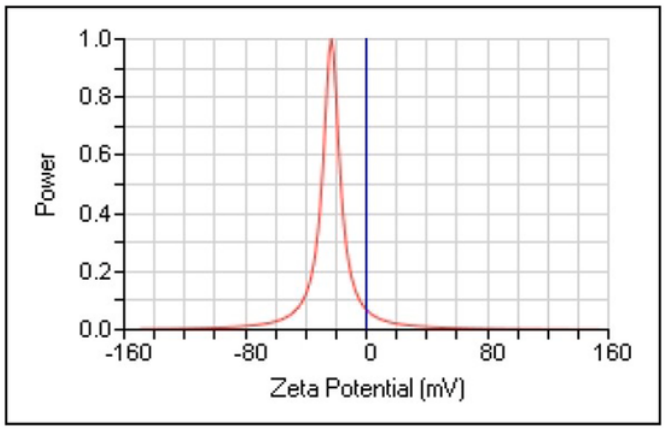

Fig. 8. Zeta potential of biosynthesized AgNPs.

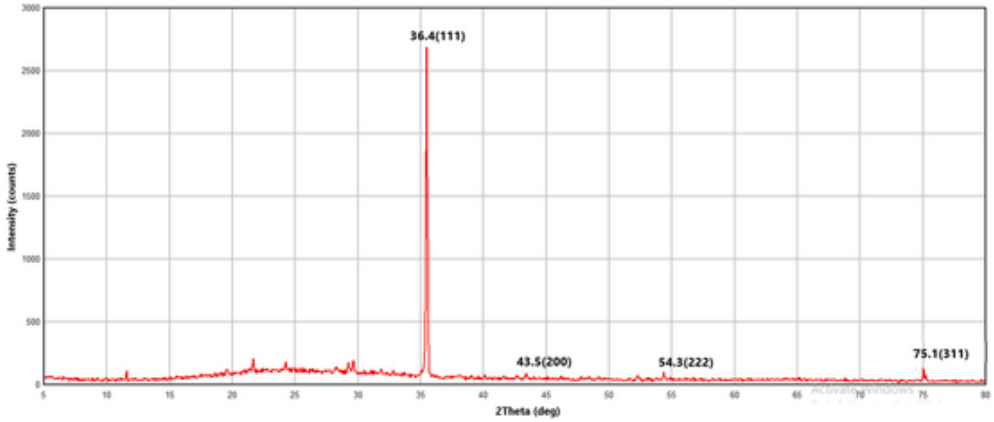

Fig. 9. The XRD pattern of biosynthesized AgNPs.

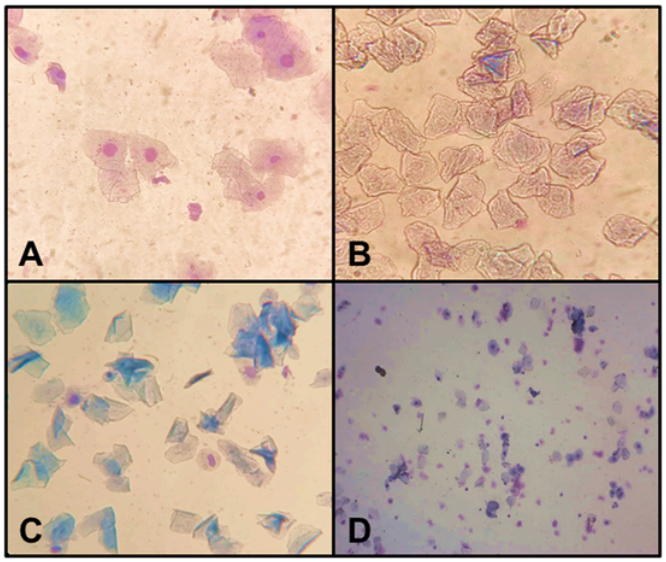

Fig. 10. Exfoliative cytology during the estrous cycle. **A)** Proestrus phase shows nucleated epithelial cells and some cornified epithelial cells, **B)** Estrus phase consists of anucleated cornified squamous epithelial cells, **C)** Metaestrus phase consist of cornified and nucleated cornified squamous epithelial cells and leukocytes, **D)** Diestrus phase consist of predominant leukocytes with few nucleated cells.

treated group) but without statistically significant differences (Fig. 11A). Apart from LH, the FSH concentration was significantly dropped in the PCOS group when compared with the vehicle control group (0.82 ± 0.09 *vs*. 0.62 ± 0.06 mIU/ml, $p < 0.001$). While in the treated groups, there were significant increases in FSH levels (metformin: 0.62 ± 0.06 *vs*. 0.74 ± 0.05 mIU/ml, $p = 0.05$; AgNPs: 0.62 ± 0.06 *vs*. 0.82 ± 0.07 mIU/ml, $p < 0.001$) when compared with the PCOS group (Fig. 11B).

In Fig. 11C, E2 serum concentration was significantly higher in the PCOS rats (untreated group) than in the control group (35.05 ± 5.43 *vs*. 20.22 ± 5.12 ng/ml, $p < 0.001$). While, it is notably decreased after treatments when compared with untreated PCOS rats (CZ: 23.58 ± 3.88 *vs*. 35.05 ± 5.43 ng/ml, $p = 0.005$; metformin: 22.73 ± 5.54 *vs*. 35.05 ± 5.43 ng/ml, $p = 0.003$; AgNPs: 25.55 ± 5.32 *vs*. 35.05 ± 5.43 ng/ml, $p = 0.02$). In comparison with the vehicle control group, Fig. 11D demonstrates that there was a significant decrease in the serum PROG of PCOS rats (51.08 ± 5.40 *vs*. 34.98 ± 6.97 ng/ml, $p = 0.002$). Whereas, it is increased after treatment with AgNPs (34.98 ± 6.97 *vs*. 46.70 ± 5.90 ng/ml, $p = 0.03$). Serum TEST concentration showed a significant increase in the PCOS group when compared with the vehicle control group (0.29 ± 0.19 *vs*. 0.78 ± 17 ng/ml, $p < 0.001$). In addition, the TEST level of group that was treated with AgNPs appears significantly decreased as compared with PCOS group (0.78 ± 17 *vs*. 0.32 ± 0.20 ng/ml, $p = 0.001$, Fig. 11E).

3.4. Reproductive efficiency

In the current study, the efficiency of 30-days' treatment was assessed by mating the female rats from different groups with healthy adult males. Table 1 illustrates that in the PCOS group only one female rat became pregnant and the weight of offspring was small, while others failed to become pregnant. Inversely, the females in the vehicle control group had a 100% pregnancy rate with an offspring weight of 5.306 ± 0.38. In PCOS females treated with CZ bark extract, metformin group and AgNPs group, all fertility para-

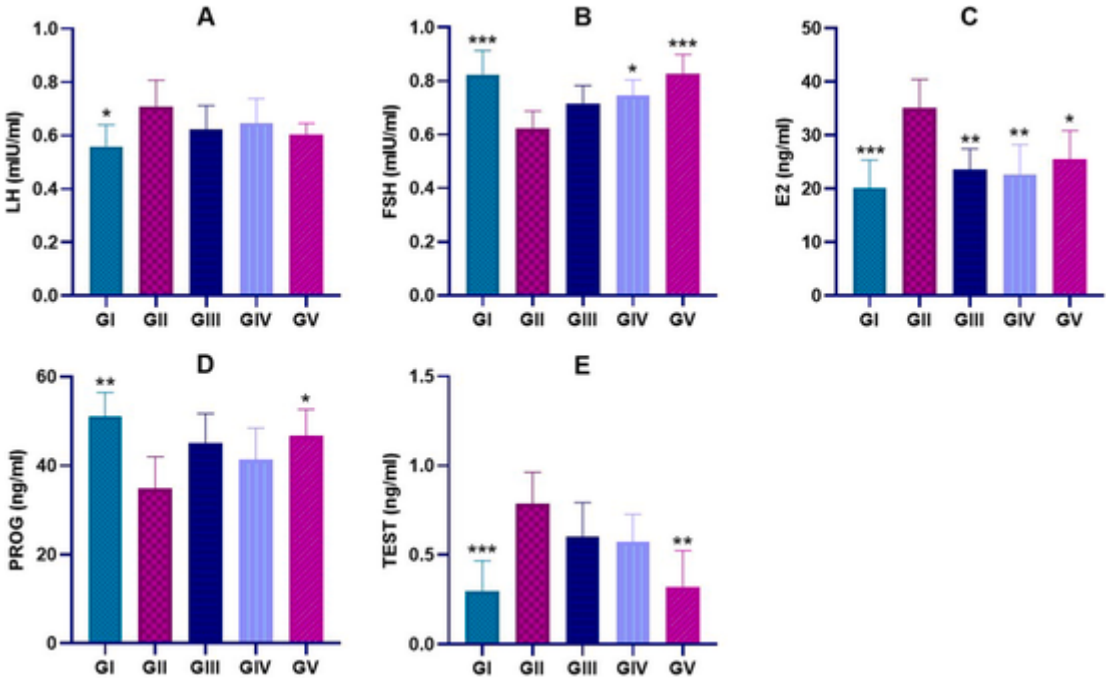

Fig. 11. The serum levels of: **A)** LH, **B)** FSH, **C)** estradiol (E2), **D)** progesterone (PROG) and **E)** testosterone (TEST). Bars represents the data as mean and SD (n = 6). * means $p \leq 0.05$, ** means $p \leq 0.01$, *** means $p \leq 0.001$ compared with the PCOS group. GI) Control group, GII) PCOS control group, GIII) group received 200 mg/kg methanolic bark extract of CZ, GIV) group received 50 mg/kg metformin, GV) group received 3.53 mg/kg biosynthesized AgNPs.

Table 1
Effects of treatments on reproductive efficiency in female rats with induced PCOS.

	GI	GII	GIII	GIV	GV	*P-value*
Pregnant rats (No.)	4/4	1/4	4/4	4/4	4/4	
Total births (No.)	45	9	42	21	36	
Wt. of offspring (g)	5.306 ± 0.38^{a}	3.75 ± 0.35^{c}	4.68 ± 0.49^{b}	4.56 ± 0.45^{b}	4.58 ± 0.56^{b}	<0.001
Deaths (No.)	0	1	0	6	0	
Fertility rate (%)	100%	25%	100%	100%	100%	

Different small letters denote significant differences at the ($p < 0.05$) level. GI) Control group, GII) PCOS control group, GIII) group received 200 mg/kg methanolic bark extract of CZ, GIV) group received 50 mg/kg metformin, GV) group received 3.53 mg/kg biosynthesized AgNPs.

meters appeared to be improved, with fertility rates of 100%. But in the group that was treated with metformin, some of the females had dystocia, so a number of offspring died.

3.5. Histopathologic features

The microscopic examinations of the ovarian tissues of the vehicle control group showed the presence of normal cellular tissue structure of the ovary with various numbers of healthy follicles at different stages of differentiation (primary, secondary and Graafian follicles) with the presence of multiple large corpus luteum (Fig. 12A). As compared with ovarian tissues of the vehicle control group, the stained section of ovary from the PCOS group showed multiple follicular cyst (FC) formation in different sizes and a decrease in the number of corpus luteum. The FCs had a thick theca cell layer and a thin granulosa cell layer with desquamation of granulosa cells within the cystic fluid (Fig. 12B). On the other hand, in the group treated with CZ bark extract the number of primary follicles and Graafian follicles (GF) normal structure follicles were observed, few were degenerated or cystic when compared with the PCOS group with the presence of corpus luteum (Fig. 12C). Fig. 12D shows the ovarian microscopic tissue features after the treatment with metformin which reveals normal histological findings of ovarian tissue with normal primary follicles and corpus luteum as well as one follicular cyst. PCOS rats treated with AgNPs show normal ovarian tissue findings with more active corpus luteum indicating restoration of ovulatory function of the ovary and of reaming of two FCs (Fig. 12E).

4. Discussion

Despite the advancement in pharmaceutical sciences, the treatment of many conditions is still challenging due to unclear etiology. However, searching for new treatments with more efficiency than the current ones is obviously necessary. In addition to the efficiency of CZ in treating PCOS (Dou et al., 2018; Heydarpour et al., 2020), previous reports have also shown that AgNPs may have a

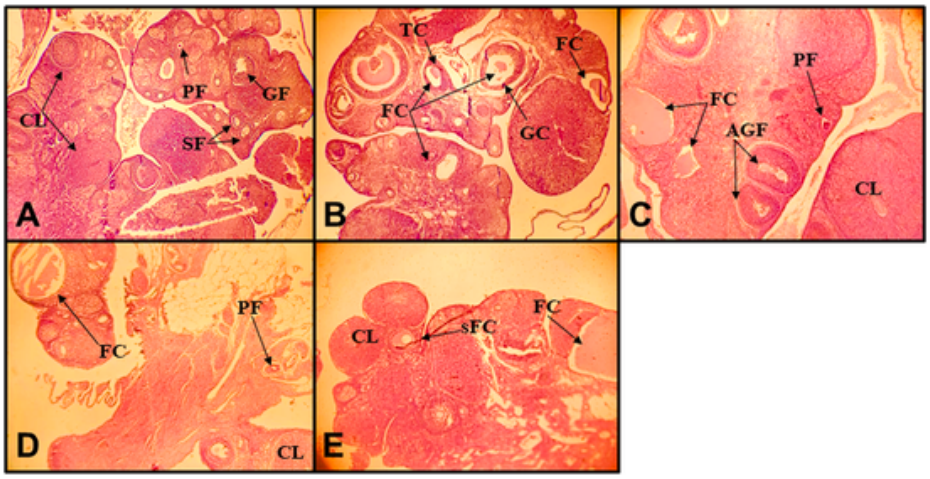

Fig. 12. Histopathological microscopic features of H&E stained slides of tissue ovaries of the experimental and the control groups (4X). **A)** Vehicle control group, **B)** positive control (PCOS) group, **C)** PCOS rats treated with CZ bark extract group, **D)** PCOS rats treated with metformin, **F)** PCOS rats treated with AgNPs. Representative images show various developing follicles (Primary follicle (PF), Secondary follicle (SF) and Graafian follicle (GF), follicular cyst (FC) in different sizes (small follicular cyst (sFC), atretic Graafian follicle (AGF), thickness granulosa cell (GC), thin theca cell (TC) and corpus luteum (CL).

good role in this respect (Salami et al., 2018). Thus, the rationale behind the current study was to explore the effects of AgNPs biofabricated by CZ bark extract since it has not yet been elucidated.

Firstly, our study uses an efficient protocol for the green or biosynthesis of AgNPs (using CZ bark extract). In this method of metallic nanoparticles' synthesis, the plant's secondary metabolites (or bioactive constituents) are utilized and act as reducing and capping agents. The color change (darkness) of the solution ($AgNO_3$ + CZ extract) indicates the fabrication of AgNPs by reducing the Ag^+ into Ag^0 via the bioactive secondary metabolites of CZ (Figs. 1 and Fig.2). This color arises due to excitation of surface plasmon vibration in AgNPs, Kumararaja et al. (2019) said. The plant extract includes various metabolites, such as phenols, flavonoids, terpenoids, proteins, and carbs that all are essential for stabilizing metallic silvers and reducing them to AgNPs (Vanaja and Annadurai, 2013). Rajesh et al. (2009) reported that reduction of Ag^+ into Ag^0NPs during the exposure to the plant extracts could result in color change. Our findings were in agreement with those of Kumararaja et al. (2019) who found that the color of biosynthesized AgNPs (using CZ) is changed to yellow, followed by brown and dark brown after 72h.

In the UV–Vis spectrum, there is a visible peak at 428 nm after 72h of incubation as shown in Fig. 3. The absorption spectrum of the pale yellow silver colloids prepared by CZ bark extract showed a surface plasmon absorption band around 400 nm, indicating the presence of one spherical or roughly spherical AgNPs (Sathishkumar et al., 2009). CZ bark extract was exposed to UV–visible spectrophotometer after 72h and a distinct peak was observed at 428 nm which is an indicator of reduction of Ag ions. These results were inline with those of Awwad et al. (2013) and Nasrollahzadeh et al. (2015). It should be noted that the position of surface plasmon resonances depends on different factors (such as size and shape). The spectra were recorded when both color and absorption intensity of the samples stayed constant. Such observation also gives preliminary prediction regarding the size and its distribution of AgNPs (Sulaiman et al., 2013). SEM, AFM and zeta-potential results showed that biosynthesized AgNPs were spherical shaped with smooth edges and nano-sizes (Figs. 4, Figs. 5 and Fig.6). Herein, our results agreed with those of Gauthami et al. (2015). The SEM analysis revealed that silver particles are present in nano-sizes. These particles were spherical, with little aggregations, and below 100 nm (ranging from 60 to 80 nm). The aggregation happens as a result of the presence of cellular components, that act as capping and reducing agents, on the surface of nanoparticles (Bélteky et al., 2019). The gained particles' sizes, in a recent work by Alsamhary (2020), were also about 60 nm determined by AFM. The FT-IR results (Fig. 7) showed the presence of various functional groups in the cinnamon's (CZ) extract. These functional groups were belonging to phenols, alcohols, alkane, alkynes, and aldehydes (particularly, cinnamaldehyde). In 2017, Salim et al. reported similar findings. The zeta potential's values of AgNPs were −23.07 (Fig. 8). The magnitude of zeta potential gives an indication of the potential stability of colloidal system. If the particles have high negative or high positive potential, they tend to repel and there will be no tendency of the particles to be together in a system. If the particles have low zeta potential values, there will be no force to prevent them to come together and flocculate. Particles with zeta potential in the range +30 mV to −30mV are considered to be stable (Gauthami et al., 2015). Furthermore, the XRD pattern (Fig. 9) obviously revealed that the biogenic nanoparticles, formed by reducing Ag^+ to Ag^0 with CZ extracts, are crystalline in nature. The average crystallites sizes according to Debye–Scherrer equation was 36.4 nm for AgNPs. This agrees with the findings of Sathishkumar et al. (2009) was found clear peaks of cubic phases at 36.4 (111), 43.5 (200), 54.5 (220) and 75.1 (311). Overall, this study provides pieces of evidence that the CZ bark extract is a good way for the biosynthesis of stable AgNPs in lesser time.

Alterations in gonadotropin-releasing hormone (GnRH) levels in serum and the formation of multiple poly-cysts in the ovary can be induced in female rats by injecting them with hormones, namely estradiol valerate (EV), dihydrotestosterone (DHT), or letrozole, since the experimental PCOS in rats resembles that in humans (Azarnia et al., 2015; Reddy et al., 2016). In the current study, we induced PCOS by EV in regular cycle female rats. In the rats that received EV, vaginal smears showed a failure in cyclic reproductive mechanism as well as a variety of metabolic abnormalities linked to hormonal disturbance. The vaginal cornification with high levels

of estrogens, which are characteristics of follicular cysts FCs development, was corroborated by the histological study. The current study shows that PCOS was successfully induced in rats due to the multiple FCs and the vaginal smear cells that differ from those in regular ECs (Bhuvaneshwari et al., 2015). Several herbal therapies are available to treat PCOS, such as CZ which have a great and important effect in regulating the menstrual cycle in women with PCOS (Kort and Lobo, 2014). The results of the current study have also proven that AgNPs biofabricated using CZ can effectively restore the EC regularity (Fig. 10). Similarly, the AgNPs regulate hormones (LH, FSH, E2, PROG, and TEST) that are involved in the pathophysiology of PCOS (Fig. 11). In comparison with the control group, we found that the PCOS group had higher levels of LH and significantly dropped levels of FSH and this agreed to previous results of Mohammed et al. (2021). While, another study by Alzahrani et al. (2019) gained contrary findings regarding FSH levels and this may be due to high levels of E2 which might be one explanation for these findings. Persistent estrus maintains serum estrogen levels in PCOS rodent models and is considered to correspond to human PCOS characteristics (Kondo et al., 2016). In addition, the results for the treatment groups show a decline in the level of LH compared with the PCOS untreated group, especially in groups treated with CZ bark extract and biosynthesized AgNPs. However, the results of FSH level after treatment appear significantly increased in CZ, metformin group, and AgNPs groups. Accordingly, these findings point to the role of bioactive compounds that are found in CZ which play an important role in the treatment of PCOS and regulation of circulating hormones. Similarly, the findings of Anbu and Venkatachalam (2016) support our results. The E2 concentration in the present study shows high level in PCOS group than in the control which is similar to the results similar of Kondo et al. (2016). The experimental groups after treatment, especially those treated with the treatment with CZ, metformin, and AgNPs, have decreased E2 levels. The PROG levels decreased significantly in the PCOS group when compared with the control group. While, the experimental group that received CZ bark extract and AgNPs had higher PROG levels than in metformin-treated group. Anbu and Venkatachalam (2016) reported similar outcomes, with a significant increase in PROG levels in rats with PCOS after administration of a high dose of biomolecule-coated chitosan nanoparticles from CZ methanolic extract. Regarding TEST levels, the rats with PCOS have a significant increase. But, the rats treated with AgNPs seem to have a declined levels of testosterone. Excess androgen is a key feature of PCOS, which is observed in about 60–80% of patients (Bednarska and Siejka, 2017). According to the regular EC and restored hormonal levels after treatment, the regulatory role of AgNPs may be attributed to the cytotoxic effect of accumulated NPs that can be targeted the polycysts through apoptosis (Gao et al., 2012; Hou and Zhu, 2017).

Whereas 75% of rats with PCOS (untreated) were affected by the EV-induced polycysts and became infertile, the fertility rate of rats with PCOS after treatment (either with CZ, metformin, or AgNPs) was restored to 100%. Infertility may be resulted due to multiple ovarian cysts, irregular EC, and hormonal disturbances. PCOS which one of the most common causes of female infertility due to anovulation and hyperandrogenism that lead to ovarian dysfunctions (Chaudhari and Nampoothiri, 2017). The fertility rate was improved after treatment especially in CZ bark extract and AgNPs groups. These results clarified the role of CZ in regulating the EC and hormonal disturbances in rats with PCOS.

The hormonal findings of the current study have been strongly supported by histopathological study of ovarian tissues. In the rats with PCOS (untreated group), induction of PCOS resulted in a significant increase in the number of FCs with a very thin granulosa layer and thick theca layer and scanty corpora lutea were detected. While the number of primary, secondary and Graafian follicles were significantly decreased as compared with the vehicle control group, which is consistent with previous findings by Jelodar et al. (2018). Also, this is in agreement with the results of Ghafurniyan et al. (2015) who reported a low number of corpora lutea, indicating that EV injection-induced polycystation reduced active follicle showing anovulation and the frequency of EC is totally absent in PCOS rats. Alternatively, this result may be due to a sudden increase in LH levels, which is thought to be a vital part of the ovulation process (Jashni et al., 2016). Khodaeifar et al. (2019) revealed that treatment with hydroalcoholic extract of CZ could regulate the level of gonadotropin and steroid hormones. Eventually, the hydroalcoholic extract of CZ could decrease the number of follicular cysts and increase the number of normal follicles. These results are consistent with the findings of the current study. However, CZ effects on the prevention of FC generating can be due to the anti-hyperandrogenic properties of this herb on the rats treated with CZ bark extract and those treated with metformin. In addition, studies indicate that metformin inhibits the production of androgen by reducing pituitary LH secretion, causing ovulation and regulates menstrual cycles when acting on ovarian thecal cells (Faure et al., 2018). The histopathological findings in PCOS rats treated with AgNPs revealed a remarkable reorganization of ovarian tissue, with the development of normal follicular structure and reduction in the formation of FCs. Based on the microscopic features, the presence of number of primary, secondary and Graafian follicles were noticed and the follicles had normal granulosa with well-organized thecal cells. These were inline with the study by Anbu and Venkatachalam (2016) who reported that biomolecule-loaded chitosan NPs' treatment is responsible for functional corpora lutea formation in addition to the regularity of the EC.

Although the hypothesis was tested from different sides, however, it still subjects to certain limitations. Firstly, gene expression of the hormones involved in the pathogenesis of PCOS was not evaluated which can support our findings and aid in drawing more rigorous conclusions. Secondly, the duration of treatment and assessment of doses was limited to only 30 days, which may not provide a clear explanation about the possibility of regenerating PCOS. However, and in spite these limitations, this is the first study about the effectiveness of biosynthesized AgNPs on PCOS.

5. Conclusions

In conclusion, we designed the current study by inducing PCOS in rats by hormonal method (EV) in order to develop a PCOS model that is clinically similar to PCOS in women. Using a PCOS rat model, we studied the anti-PCOS effects of biosynthesized AgNPs. Based on the findings of the this study, biosynthesized AgNPs appear to have a powerful therapeutic effects on rats with PCOS by reg-

ulating serum sex hormone levels (LH, FSH, E2, progesterone and testosterone), regulating the estrus cycle, and improving the reproductive efficiency of rats.

Ethics approval and consent to participate

- The University of Basra, College of Veterinary Medicine approved this study and its protocols (No: 3/18-01/07/2019).

Consent for publication

- N/A.

Availability of data and material

- Upon reasonable request, the data associated with this paper can be requested from the corresponding author Shukrya Alwan.

Funding

- The authors themselves funded the current study, with no external funding.

Authors' contributions

- **SA** designed the study, prepared the manuscript, and did the practical part of this work. **MA** supervised the practical part of this project and reviewed the manuscript. **SA** and **MA** authors have reviewed and approved the final version of the manuscript.

Ethical and acknowledgments statements

Mentioned at the end of the manuscript, just before the references.

Uncited references

Salim et al., 2017.

Declaration of competing interest

- The authors have no conflict of interest.

On behalf of all co-authors listed on my manuscript's title page, I affirm that we all have no conflict of interest.
We also affirmed this at the manuscript.

Acknowledgements

The authors would like to thank Dr. Labeeb Ahmed and Dr. Suha Mohamed (Ministry of Science and Technology, Directorate of Environment and Water) for their kind assistance in the preparation of silver nanoparticles and their characterization. They also would like to extremely thank Dr. Hussein A. Abid and Dr. Hamid K. Ali for their valuable suggestions as reviewers for the manuscript and in statistical analyses. Finally, big thanks to Mr. Hatem Mohammed for his contribution to working at the animal house.

Abbreviations

AFM	atomic force microscopy
$AgNO_3$	silver nitrate
AgNPs	Silver nanoparticles
BMI	body mass index
CZ	*Cinnamomum zeylanicum*
AgNPs	silver nanoparticles of *C. zeylanicum* methanol bark extract
DM	diabetes mellitus
EV	estradiol valerate
FC	follicular cyst
FSH	follicle-stimulating hormone
FTIR	Fourier transforms infrared spectroscopy analysis
GF	Graafian follicles
IR	insulin resistance
LH	luteinizing hormone
PCOM	polycystic ovarian morphology
PCOS	Polycystic ovarian syndrome
SEM	scanning electron microscopy
XRD	X-ray diffraction

References

Abasian, Z., Rostamzadeh, A., Mohammadi, M., Hosseini, M., Rafieian-kopaei, M., 2018. A review on role of medicinal plants in polycystic ovarian syndrome: pathophysiology, neuroendocrine signaling, therapeutic status and future prospects. Middle East Fertil. Soc. J. 23, 255–262. https://doi.org/10.1016/j.mefs.2018.04.005.

Abbasi, E., Milani, M., Aval, S.F., Kouhi, M., Akbarzadeh, A., Nasrabadi, H.T., Nikasa, P., Joo, S.W., Hanifehpour, Y., Nejati-Koshki, K., Samiei, M., 2016. Silver nanoparticles: synthesis methods, bio-applications and properties. Crit. Rev. Microbiol. 42, 173–180. https://doi.org/10.3109/1040841X.2014.912200.

Abdalla, K.H., Al-Hannan, F., Alghamdi, A., Henari, F.Z., 2015. Green synthesis of silver nanoparticles using cinnamon (Cinnamomum cassia), characterization and antibacterial activity. Int. J. Sci. Res. 6, 2319–7064. https://doi.org/10.21275/ART20174199.

Alsamhary, K.I., 2020. Eco-friendly synthesis of silver nanoparticles by Bacillus subtilis and their antibacterial activity. Saudi J. Biol. Sci. 27, 2185–2191. https://doi.org/10.1016/j.sjbs.2020.04.026.

Alwan, S., Al-Saeed, M., Abid, H., 2021. Safety assessment and biochemical evaluation of the effect of biogenic silver nanoparticles (using bark extract of C. zeylanicum) on Rattus norvegicus rats. Baghdad J. Biochem. Appl. Biol. Sci. 2, 138–150. https://doi.org/10.47419/bjbabs.v2i03.67.

Alzahrani, A.A., Alahmadi, A.A., Ali, S.S., Alahmadi, B.A., Arab, R.A., Wahman, L.F., El-Shitany, N.A., 2019. Biochemical and histological evidence of thyroid gland dysfunction in estradiol valerate model of the polycystic ovary in Wistar rats. Biochem. Biophys. Res. Commun. 514, 194–199. https://doi.org/10.1016/j.bbrc.2019.04.126.

Anbu, A.S., Venkatachalam, P., 2016. Biological macromolecule cross linked TPP-chitosan complex: a novel nanohybrid for improved ovulatory activity against PCOS treatment in female rats. RSC Adv. 6, 94301–94313. https://doi.org/10.1039/c6ra07228c.

Awwad, A.M., Salem, N.M., Abdeen, A.O., 2013. Biosynthesis of silver nanoparticles using olea europaea leaves extract and its antibacterial activity. Nanosci. Nanotechnol. 2, 164–170. https://doi.org/10.5923/j.nn.20120206.03.

Azarnia, M., Sz, K., Sg, M., Saeidnia, S., 2015. Effect of hydroalcoholic extract of Melia azedarach L . seeds on serum concentration of sex hormones in polycystic ovary syndrome induced in female wistar rats Abstract : background : polycystic ovary syndrome (PCOS) is one of the most common hormonal d. KAUMS J. (FEYZ) 19, 111–117.

Azziz, R., Carmina, E., Chen, Z., Dunaif, A., Laven, J.S.E., Legro, R.S., Lizneva, D., Natterson-Horowtiz, B., Teede, H.J., Yildiz, B.O., 2016. Polycystic ovary syndrome. Nat. Rev. Dis. Prim. 2. https://doi.org/10.1038/nrdp.2016.57.

Bednarska, S., Siejka, A., 2017. The pathogenesis and treatment of polycystic ovary syndrome: what's new? Adv. Clin. Exp. Med. 26, 359–367. https://doi.org/10.17219/acem/59380.

Bélteky, P., Rónavári, A., Igaz, N., Szerencsés, B., Tóth, I.Y., Pfeiffer, I., Kiricsi, M., Kónya, Z., 2019. Silver nanoparticles: aggregation behavior in biorelevant conditions and its impact on biological activity. Int. J. Nanomed. 14, 667–687. https://doi.org/10.2147/IJN.S185965.

Bhuvaneshwari, S., Poornima, R., Averal, H.I., 2015. Detection of polycystic ovary syndrome and its treatment with pergularia daemia in rat models. IOSR J. Pharm. 5, 42–49.

Burduşel, A.-C., Gherasim, O., Grumezescu, A.M., Mogoantă, L., Ficai, A., Andronescu, E., 2018. Biomedical applications of silver nanoparticles: an up-to-date overview. Nanomaterials 8, 681. https://doi.org/10.3390/nano8090681.

Chaudhari, N.K., Nampoothiri, L.P., 2017. Neurotransmitter alteration in a testosterone propionate-induced polycystic ovarian syndrome rat model. Horm. Mol. Biol. Clin. Invest. 29, 71–77. https://doi.org/10.1515/hmbci-2016-0035.

Dorri, M., Hashemitabar, S., Hosseinzadeh, H., 2018. Cinnamon (Cinnamomum zeylanicum) as an antidote or a protective agent against natural or chemical toxicities: a review. Drug Chem. Toxicol. 41, 338–351. https://doi.org/10.1080/01480545.2017.1417995.

Dou, L., Zheng, Y., Li, L., Gui, X., Chen, Y., Yu, M., Guo, Y., 2018. The effect of cinnamon on polycystic ovary syndrome in a mouse model. Reprod. Biol. Endocrinol. 16, 1–10. https://doi.org/10.1186/s12958-018-0418-y.

Duleba, A.J., 2012. Medical management of metabolic dysfunction in PCOS. Steroids 77, 306–311. https://doi.org/10.1016/j.steroids.2011.11.014.

Faure, M., Bertoldo, M.J., Khoueiry, R., Bongrani, A., Brion, F., Giulivi, C., Dupont, J., Froment, P., 2018. Metformin in reproductive biology. Front. Endocrinol. (Lausanne) 9, 1–12. https://doi.org/10.3389/fendo.2018.00675.

Gao, G., Ze, Y., Li, B., Zhao, X., Zhang, T., Sheng, L., Hu, R., Gui, S., Sang, X., Sun, Q., Cheng, J., Cheng, Z., Wang, L., Tang, M., Hong, F., 2012. Ovarian dysfunction and gene-expressed characteristics of female mice caused by long-term exposure to titanium dioxide nanoparticles. J. Hazard Mater. 243, 19–27. https://doi.org/10.1016/j.jhazmat.2012.08.049.

Gauthami, M., Srinivasan, N., M. Goud, N., Boopalan, K., Thirumurugan, K., 2015. Synthesis of silver nanoparticles using Cinnamomum zeylanicum bark extract and its antioxidant activity. Nanosci. Nanotechnol. - Asia 5, 2–7. https://doi.org/10.2174/2210681205011507281032O9.

Ghafurniyan, H., Azarnia, M., Nabiuni, M., Karimzadeh, L., 2015. The effect of green tea extract on reproductive improvement in estradiol valerate-induced polycystic ovary polycystic ovarian syndrome in rat. Iran. J. Pharm. Res. 14, 1215–1223. https://doi.org/10.22037/ijpr.2015.1728.

Gurunathan, S., Park, J.H., Han, J.W., Kim, J.-H., 2015. Comparative assessment of the apoptotic potential of silver nanoparticles synthesized by Bacillus tequilensis and Calocybe indica in MDA-MB-231 human breast cancer cells: targeting p53 for anticancer therapy. Int. J. Nanomed. 10, 4203–4222. https://doi.org/10.2147/IJN.S83953.

Heydarpour, F., Hemati, N., Hadi, A., Moradi, S., Mohammadi, E., Farzaei, M.H., 2020. Effects of cinnamon on controlling metabolic parameters of polycystic ovary syndrome: a systematic review and meta-analysis. J. Ethnopharmacol. 254. https://doi.org/10.1016/j.jep.2020.112741.

Hou, C.-C., Zhu, J.-Q., 2017. Nanoparticles and female reproductive system: how do nanoparticles affect oogenesis and embryonic development. Oncotarget 8, 109799–109817. https://doi.org/10.18632/oncotarget.19087.

Ingale, A.G., Chaudhari, A.N., 2013. Biogenic synthesis of nanoparticles and potential applications: an eco-friendly approach. J. Nanomed. Nanotechnol. 4, 7. https://doi.org/10.4172/2157-7439.1000165.

Jashni, H.K., Kargar Jahromi, H., Bagheri, Z., 2016. The effect of palm pollen extract on polycystic ovary syndrome (POS) in rats. Int. J. Med. Res. Health Sci. 5, 317–321. www.ijmrhs.com.

Jasim, N.A., Al-Gasha'a, F.A., Al-Marjani, M.F., Al-Rahal, A.H., Abid, H.A., Al-Kadhmi, N.A., Jakaria, M., Rheima, A.M., 2020. ZnO nanoparticles inhibit growth and biofilm formation of vancomycin-resistant S. aureus (VRSA). Biocatal. Agric. Biotechnol. 29. https://doi.org/10.1016/j.bcab.2020.101745.

Jelodar, G., Masoomi, S., Rahmanifar, F., 2018. Hydroalcoholic extract of flaxseed improves polycystic ovary syndrome in a rat model. Iran. J. Basic Med. Sci. 21, 645–650. https://doi.org/10.22038/ijbms.2018.25778.6349.

Keshari, A.K., Srivastava, R., Singh, P., Yadav, V.B., Nath, G., 2020. Antioxidant and antibacterial activity of silver nanoparticles synthesized by Cestrum nocturnum. J. Ayurveda Integr. Med. https://doi.org/10.1016/j.jaim.2017.11.003.

Khodaeifar, F., Fazljou, S.M.B., Khaki, A.A.A., Torbati, M., Madarek, E.O.S., Khaki, A.A.A., Shokoohi, M., Dalili, A.H., 2019. The effect of hydroalchoholic extract of cinnamon zeylanicum on oxidative damages and biochemical change in adult rats with polycystic ovary syndrome. Crescent J. Med. Biol. Sci. 6, 511–516.

Kondo, M., Osuka, S., Iwase, A., Nakahara, T., Saito, A., Bayasula, Nakamura, T., Goto, M., Kotani, T., Kikkawa, F., 2016. Increase of kisspeptin-positive cells in the hypothalamus of a rat model of polycystic ovary syndrome. Metab. Brain Dis. 31, 673–681. https://doi.org/10.1007/s11011-016-9807-0.

Kort, D.H., Lobo, R.A., 2014. Preliminary evidence that cinnamon improves menstrual cyclicity in women with polycystic ovary syndrome: a randomized controlled trial. Am. J. Obstet. Gynecol. 211, 487.e1-487.e6. https://doi.org/10.1016/j.ajog.2014.05.009.

Kumararaja, G., Sundaraganapathy, R., Constantine, I., Vijayalakshmi, V., Fuzail, S., Rahim, A., 2019. Comparative studies on synthesized silver nanoparticles using Artemisia vulgaris Linn., and Cinnamomum zeylanicum Nees., for their antifungal activity. J. Pharmaceut. Sci. Res. 11, 2558–2565.

Mariappan, P.M., Sabesan, G., Koilpillai, B., Janakiraman, S., Sharma, N.K., 2013. Chemical characterisation and antifungal activity of methanolic extract of Cinnamomum verum. J. Presl bark against Malassezia spp. Pharmacogn. J. 5, 197–204. https://doi.org/10.1016/j.phcgj.2013.09.001.

Matsuzaki, T., Tungalagsuvd, A., Iwasa, T., Munkhzaya, M., Yanagihara, R., Tokui, T., Yano, K., Mayila, Y., Kato, T., Kuwahara, A., Matsui, S., 2017. Kisspeptin mRNA expression is increased in the posterior hypothalamus in the rat model of polycystic ovary syndrome. Endocr. J. 64, 7–14.

Mohammed, S., Sundaram, V., Zyuzikov, N., 2021. Effect of 150 kHz electromagnetic radiation on the development of polycystic ovaries induced by estradiol Valerate in Sprague Dawley rats. J. Ovarian Res. 14, 1–10. https://doi.org/10.1186/s13048-021-00774-4.

Nasrollahzadeh, M., Sajadi, M.M., Babaei, F., Maham, M., 2015. Euphorbia helioscopia Linn as a green source for synthesis of silver nanoparticles and their optical and catalytic properties. J. Colloid Interface Sci. 450, 374–380. https://doi.org/10.1016/j.jcis.2015.03.033.
Nasser, H.A., Ezz, N.Z.A., Abdel-Mageed, H.M., Radwan, R.A., 2019. Body mass index and C-reactive protein are potential predictors of asthma development in Egyptian polycystic ovary syndrome patients. J. Med. Biochem. 38, 427–436. https://doi.org/10.2478/jomb-2019-0012.
Parveen, A., Rao, S., 2015. Mechanistic approach of functionalized noble metal nanoparticles synthesis from Cassia auriculata L. J. Cluster Sci. 26, 1295–1303. https://doi.org/10.1007/s10876-014-0813-2.
Rajesh, R.W., Jaya, L.R., Niranjan, K.S., Vijay, D.M., Sahebrao, B.K., 2009. Phytosynthesis of silver nanoparticle using gliricidia sepium (Jacq.). Curr. Nanosci. 5, 117–122.
Ranasinghe, P., Pigera, S., Premakumara, G.S., Galappaththy, P., Constantine, G.R., Katulanda, P., 2013. Medicinal properties of "true" cinnamon (Cinnamomum zeylanicum): a systematic review. BMC Compl. Alternative Med. 13. https://doi.org/10.1186/1472-6882-13-275.
Reddy, P.S., Begum, N., Mutha, S., Bakshi, V., 2016. Asian paci fi c journal of reproduction. Asian Pacific J. Reprod. 5, 116–122. https://doi.org/10.1016/j.apjr.2016.01.006.
Rosenfield, R.L., Ehrmann, D.A., 2016. The Pathogenesis of Polycystic Ovary Syndrome (PCOS): the hypothesis of PCOS as functional ovarian hyperandrogenism revisited. Endocr. Rev. 37, 467–520. https://doi.org/10.1210/er.2015-1104.
Rostamtabar, M., Esmaeilzadeh, S., Tourani, M., Rahmani, A., Baee, M., Shirafkan, F., Saleki, K., Mirzababayi, S.S., Ebrahimpour, S., Nouri, H.R., 2021. Pathophysiological roles of chronic low-grade inflammation mediators in polycystic ovary syndrome. J. Cell. Physiol. 236, 824–838. https://doi.org/10.1002/jcp.29912.
Salami, E., Karami, M., Dehkordi, A.J., Nadoushan, M.J., Hajnorouzi, A., 2018. Protective effect of silver nano particles against ovarian polycystic induced by morphine in rat. Nanomedicine Res. J. 3, 229–235. https://doi.org/10.22034/NMRJ.2018.04.007.
Salim, A.A., Bidin, N., Lafi, A.S., Huyop, F.Z., 2017. Antibacterial activity of PLAL synthesized nanocinnamon. Mater. Des. 132, 486–495. https://doi.org/10.1016/j.matdes.2017.07.014.
Sankar, R., Karthik, A., Prabu, A., Karthik, S., Shivashangari, K.S., Ravikumar, V., 2013. Origanum vulgare mediated biosynthesis of silver nanoparticles for its antibacterial and anticancer activity. Colloids Surf. B Biointerfaces 108, 80–84. https://doi.org/10.1016/j.colsurfb.2013.02.033.
Sathishkumar, M., Sneha, K., Won, S.W., Cho, C.W., Kim, S., Yun, Y.S., 2009. Cinnamon zeylanicum bark extract and powder mediated green synthesis of nano-crystalline silver particles and its bactericidal activity. Colloids Surf. B Biointerfaces 73, 332–338. https://doi.org/10.1016/j.colsurfb.2009.06.005.
Sriramulu, M., Sumathi, S., 2017. Photocatalytic, antioxidant, antibacterial and anti-inflammatory activity of silver nanoparticles synthesised using forest and edible mushroom. Adv. Nat. Sci. Nanosci. Nanotechnol. https://doi.org/10.1088/2043-6254/aa92b5.
Sulaiman, G.M., Mohammed, W.H., Marzoog, T.R., Al-Amiery, A.A.A., Kadhum, A.A.H., Mohamad, A.B., 2013. Green synthesis, antimicrobial and cytotoxic effects of silver nanoparticles using Eucalyptus chapmaniana leaves extract. Asian Pac. J. Trop. Biomed. 3, 58–63. https://doi.org/10.1016/S2221-1691(13)60024-6.
Teede, H., Moran, L., Deeks, A., Chambers, D., 2008. Polycystic ovary syndrome. Aust. Dr. 25–32.
Vanaja, M., Annadurai, G., 2013. Coleus aromaticus leaf extract mediated synthesis of silver nanoparticles and its bactericidal activity. Appl. Nanosci. 3, 217–223. https://doi.org/10.1007/s13204-012-0121-9.
Wong-Ng, W., McMurdie, H.F., Hubbard, C.R., Mighell, A.D., 2001. JCPDS-ICDD research associateship (cooperative program with NBS/NIST). J. Res. Natl. Inst. Stand. Technol. 106, 1013–1028. https://doi.org/10.6028/jres.106.052.
Yaseen, S.M., Abid, H.A., Kadhim, A.A., Aboglida, E.E., 2020. Antibacterial activity of palm heart extracts collected from Iraqi Phoenix dactylifera L. J. Technol. 1, 52–59. https://doi.org/10.51173/jt.v1i1.70.